ResearchGate

See discussions, stats, and author profiles for this publication at: https://www.researchgate.net/publication/24042289

A New Approach to Quantify Spatial Distribution of Biofilm Kinetic Parameters by In Situ Determination of Oxygen Uptake Rate (OUR)

ARTICLE *in* ENVIRONMENTAL SCIENCE AND TECHNOLOGY · MARCH 2009

Impact Factor: 5.33 · DOI: 10.1021/es802373q · Source: PubMed

CITATIONS
11

READS
53

6 AUTHORS, INCLUDING:

Xiaohong Zhou
Tsinghua University
37 PUBLICATIONS **182** CITATIONS
SEE PROFILE

Hanchang Shi
Tsinghua University
158 PUBLICATIONS **2,022** CITATIONS
SEE PROFILE

Qiang Cai
Tsinghua University
39 PUBLICATIONS **175** CITATIONS
SEE PROFILE

Available from: Xiaohong Zhou
Retrieved on: 31 January 2016

Environmental Science & Technology

Subscriber access provided by TSINGHUA UNIV

Article

A New Approach to Quantify Spatial Distribution of Biofilm Kinetic Parameters by In Situ Determination of Oxygen Uptake Rate (OUR)

Xiao-Hong Zhou, Yu-Qin Qiu, Han-Chang Shi, Tong Yu, Miao He, and Qiang Cai

Environ. Sci. Technol., **2009**, 43 (3), 757-763• DOI: 10.1021/es802373q • Publication Date (Web): 22 December 2008

Downloaded from http://pubs.acs.org on March 11, 2009

More About This Article

Additional resources and features associated with this article are available within the HTML version:

- Supporting Information
- Access to high resolution figures
- Links to articles and content related to this article
- Copyright permission to reproduce figures and/or text from this article

View the Full Text HTML

ACS Publications
High quality. High impact.

Environmental Science & Technology is published by the American Chemical Society. 1155 Sixteenth Street N.W., Washington, DC 20036

Environ. Sci. Technol. **2009,** *43,* 757–763

A New Approach to Quantify Spatial Distribution of Biofilm Kinetic Parameters by In Situ Determination of Oxygen Uptake Rate (OUR)

XIAO-HONG ZHOU,[†] YU-QIN QIU,[†] HAN-CHANG SHI,*[,†] TONG YU,[‡] MIAO HE,[†] AND QIANG CAI[†]

Department of Environmental Science and Engineering, Tsinghua University, Beijing 100084, China. Department of Civil and Environmental Engineering, University of Alberta Edmonton, Canada T6G 2W2

Received April 27, 2008. Accepted November 4, 2008.

In order to guide the rational optimization of biofilm reactor design and operation in wastewater treatment, it is essential to comprehend the biokinetic behavior of microorganisms, especially with its depth variation, in biofilms. However, no fast and accurate methods have been established for measuring the stratification of biokinetic parameters in biofilm systems up to now. In this paper, a new approach was presented to quantify the spatial distribution of biokinetic parameters in biofilms with a result demonstration. A multispecies biofilm at endogenous respiration was subjected to a pulse of substrates at various locations. An oxygen microelectrode structurally combined with an additional micropipette for substrate injection was constructed to monitor the in situ OUR (oxygen uptake rate) by measuring the dissolved oxygen concentration with time. Based on the oxygen concentration profiles versus times at a series of substrate concentrations, the spatial distribution of biokinetic parameters, biomass yield coefficient (Y_H), Monod half-saturation coefficient for substrate ($K_{H,S}$), and maximum specific growth rate ($\mu_{H,max}$) were quantified. The demonstration of its utility showed that Y_H was within the 0.437−0.449 g (COD in cell)/g COD range, with only a slight difference and no regular change in the spatial distribution. Meanwhile, the results showed that the distribution of $\mu_{H,max}$ varied from 9.18 day^{-1} at the surface layer of the biofilm to 1.69 day^{-1} at the substratum layer of the biofilm with a decrease of 80% due to the reduction of biomass activity or the diverse distribution of microbial species. Additionally, an opposite change tendency of $K_{H,S}$ was found, which increased from 37 mg COD/L at the surface layer of the biofilm to 45 mg COD/L at the substratum layer of the biofilm, indicating larger mass transport limitations with penetration into the biofilm. Compared with high heterogeneity in the biofilm depth, the distribution of biokinetic parameters was less heterogeneous in the horizontal direction at the same depth. In summary, the results provide experimental evidence necessary for biofilm modeling, which could not be accomplished in the past, and enable us to obtain a clearer biokinetic description of the biofilm.

* Corresponding author phone: 86-10-62773095; fax: 86-10-62771472; e-mail: hanchang@mail.tsinghua.edu.cn.
[†] Tsinghua University.
[‡] University of Alberta Edmonton.

Introduction

There is growing recognition of the importance of both natural and artificial biofilms in wastewater treatment. Biofilm systems have several advantages over conventional activated sludge plants, including the ability to support a variety of microbial populations at various locations within the biofilm which may degrade different organic substrates, and the sequestering ability of the glycocalyx surrounding the microorganisms which protects them from harmful toxicants (*1*).

Understanding the biodegradation kinetics of biofilms is essential for the rational optimization of biofilm reactor design and operation. However, the biokinetic parameters are particularly difficult to be measured because diffusional resistance within the biofilm would likely mask its true reaction kinetics (*2*). Respirometric technique, based on the determination of the respiration rate of microorganisms (oxygen uptake rate, OUR), has been commonly used to quantify microbial growth, associated substrate depletion, and product formation in activated sludge (*3*−*6*). Recently, some researchers have also determined the OUR in biofilm reactors to quantify the biokinetic parameters in biofilm systems (*7*−*9*). These studies have nonnegligible drawbacks, although these results can reflect the diffusional mass transport limitations. First, all conclusions are based on the assumption that oxygen is not the growth limiting factor. However, it is obviously difficult to justify it due to the oxygen diffusional limitation in biofilm systems. Second, the failure of assumptions, such as on uniform biofilm thickness, density, structure, and completely mixed bulk liquid, could result in the failure of these methods, although these assumptions are in contrast to the heterogeneity of biofilms in that highly complex structures containing voids, connecting channels between these voids, and microbial clusters or layers with nonuniform spatial distribution of biofilm properties such as density, porosity, and effective diffusivity, were found recently to be predominant in multispecies of biofilms (*10, 11*). The drawbacks lead to the facts that the stratified biokinetic parameters cannot be taken into consideration and acquired in the past studies.

Rapid advances in microelectrode technology have permitted in situ chemical characterization of the microbial community. Many studies have focused on the measurement of biokinetic parameters of biofilm using microelectrodes based on the well-known reaction-diffusion equation (*12*−*15*). However, to the best of our knowledge, the reported studies are still based on assumptions of the biofilm's uniform structure. Little work has been done to quantify the biokinetic parameters with respect to the structural heterogeneity in biofilms. The aim of this study, therefore, is to propose a new approach to acquire the spatial distribution of biokinetic parameters in biofilms. The approach is based on the in situ determination of OUR by the introduction of oxygen microelectrode so to reveal the stratified biodegradation kinetics of biofilms.

Materials and Methods

2.1. Biofilm. The support material for biofilm was a piece of flat polymerized ethylene resin with an area of 30 × 30 mm. One side of the resin was rubbed coarse to make the bacterial inoculation easier. The introduced activated sludge was taken from a bench-scale oxidation ditch. After one day of inoculation, the introduced activated sludge was completely withdrawn. Subsequently, eight pieces of support material were immersed in a 2.5 L reactor, and the biofilm

10.1021/es802373q CCC: $40.75 © 2009 American Chemical Society
Published on Web 12/22/2008

TABLE 1. Water Quality of Domestic Wastewater

items	concentration (mg/L[a])
COD	300∼400
NH_3−N	25∼40
TN	30∼45
SS	7∼82
pH	6.5∼8.0

[a] Except pH.

was statically cultured with domestic wastewater from the drainage of Tsinghua University Campus (see Table 1) at a room temperature of 18 ± 2 °C. Air from the gas blower was introduced to the reactor to maintain an oxygen concentration of about 5−6 mg/L through a frosted aerator. The domestic wastewater in the reactor was shifted every 12 h. After 2−3 months of operation, the biofilm with a depth of 1−2 mm was ready for the microelectrode measurement.

2.2. Microslicing Technique for the Measurement of Depth Variation of Biofilm Densities. The spatial distribution of layer densities in the biofilm was acquired using microslicing technique as similar as reported by Taylor et al. (*38*). A biofilm sample with an area of approximately 1.5 × 1.5 cm cut from the support media with a blade was attached to a cutting stage with Tissue-Tek OCT 4583 freezing compound (Miles, Inc., Pittsburgh, PA). Biofilm was sliced parallel to its surface using a LEICA CM1900 (Leica, German) cryostatic microtome. The biofilm sample was cut in slices with 50 μm thickness. Two adjacent slices were accumulated (totaling 100 μm), and then transferred to a 5 mL microcentrifuge tube filled with normal saline solution (0.85% NaCl). It should be noted that we compared the biofilm thickness measured by the microslicing technique and by the microelectrode (*11*) to evaluate the effect of freezing compound on the thickness of biofilm, and found that the total biofilm thickness measured by microslicing technique was approximately in accordance with the result measured by microelectrode. In addition, to meet the precision of electronic balance (0.1 mg), the biofilm slices from 20 biofilm samples at the same biofilm depth were accumulated into one tube. The layer density of biofilm was determined by the standard dry weight measurement (*37*). The dry cell mass, in terms of volatile solids (W_d, g VS), was measured from the difference in weights after drying at 105 °C overnight and after combustion at 550 °C for 2 h.. The wet biofilm volume (V_f, L) at each layer was calculated from the biofilm thickness (100 μm) and the biofilm area of 15 × 15 mm × 20, therefore the experimental layer density of biofilm (X_f, g COD/L) was calculated as $X_f = W_d / V_f \times 1.42$ g COD/g VS with an empirical cell formulation of $C_5H_7O_2N$. Eventually, the stratified biofilm densities measured along the depth were implemented in the following modeling.

2.3. Microelectrode for OUR Determination. A new structure of oxygen microelectrode was constructed in order to monitor the in situ OUR in biofilms. The basic component was a separated oxygen microelectrode with a tip diameter of about 10 μm as described by Yu (*16*). The sensors have a quick response time of less than 5 s, and all had insignificant stirring sensitivity (less than 5%). Apart from that, an assistant micropipette with a tip diameter of about 50 μm was pulled for the in situ addition of carbon substrate. The two micropipettes were inserted into an outer casing made of a pasture pipet (Corning Pasteur Pipette, 5.57in long, Sigma-Aldrich). Utilizing a microscope, the distance of between the two tips was adjusted to be not further than 100 μm. To make the microelectrode signal steadier, the space between the pipettes and the outer casing was filled with 1 mol/L KCl solution (*17*). A chlorinated silver wire inserted into the outer electrolyte was connected to the ground plug on the switch.

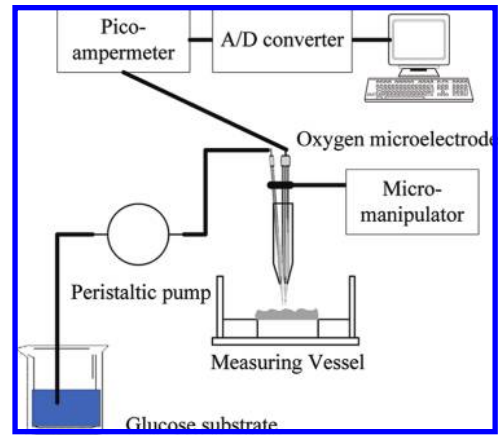

FIGURE 1. Schematic diagram of experimental setup for microelectrode measurement.

2.4. Microelectrode Measurements. The schematic diagram of experimental setup for the in situ microelectrode measurement of OUR in biofilms is shown in Figure 1. The measuring vessel for biofilms was made of polymerized ethylene resin (area of 60 × 60 mm and height of 20 mm) with a hollow interior for affixing the biofilm substratum (30 × 30 mm × 5 mm). An Ag/AgCl/saturated KCl electrode (RuoSull Technology CO., LTD, Shanghai, no. 218) was used as reference and was immersed in the vessel solution. The signals, current for the oxygen microelectrode, were transmitted by isolated wires to the pico-amperometer (PA2000, Unisense, Denmark). Data acquisition and visualization were performed by using an A/D converter (UA303, Beijing YouCai Monitoring Company, China) and data acquisition software, which resulted in the display of concentration profiles in real time on a computer. Each microelectrode was mounted on and controlled by a motor-driven micromanipulator (Beijing Micor/Nano Laser Equipment Co., Ltd., China, with precisions of 5 and 10 μm in the *z*-axis and *x*- and *y*-axes, respectively). To minimize the ambient interference, the measuring vessel, shielded by a Faraday cage (40 × 60 cm in area, 60 cm in height), was placed on a vibration isolation table (Meiritsu Seiki CO., LTD, Japan, AVT-0806S). All measurements were conducted at a room temperature of 18 ± 2 °C.

The biofilm taken from the wastewater reactor was placed in the measuring vessel, covered with the deionized water, and allowed to stand for over 24 h before the injection of a substrate solution. When the biofilm was at the endogenous phase of respiration, a dose of carbon solution with predetermined concentration was injected by a peristaltic pump into the biofilm. The selected carbon substrate was glucose with concentrations of 1.6 mg COD/L, 3.2 mg COD/L, 4.8 mg COD/L, 6.4 mg COD/L, and 8 mg COD/L, respectively. The injection time was set at 6 s. At each concentration, oxygen consumption measurements were conducted at a fixed position, starting approximately at a depth of 100 μm at the surface layer of biofilm and continuing on to the bottom with measurement intervals of 100 μm. To obtain the heterotrophic biokinetic parameters, the inhibitor for suppressing OUR of nitrification, allythiourea (ATU), was added to the substrate solution with a final concentration of 5 mg/L (*5*).

Results and Discussion

3.1. Dissolved Oxygen Profile with Time in Biofilm. A representative plot of dissolved oxygen concentration (S_O, mg DO/L) profile with time, which was measured before and after the injection of glucose with a concentration of 6.4 mg COD/L at the biofilm depth of 800 μm, is shown in

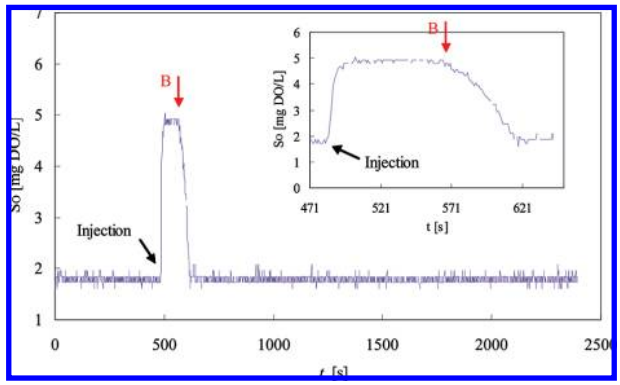

FIGURE 2. Typical oxygen concentration profile with time before and after the injection of glucose solution in biofilm, in which point B indicated by arrow means the moment of a sharp decreasing in oxygen concentration.

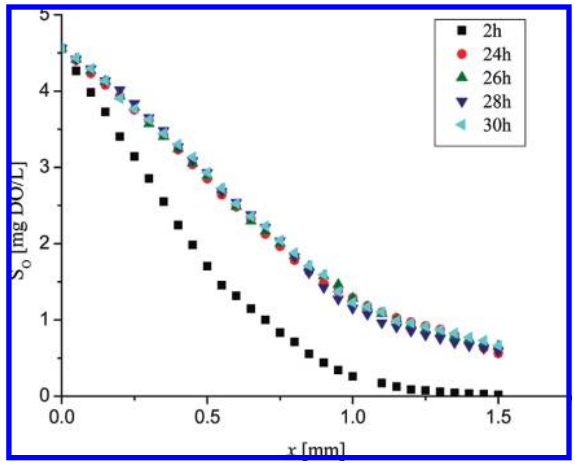

FIGURE 3. Oxygen concentration depth profiles measured at the different retention times in the biofilm covered with the deionized water.

Figure 2. It can be seen that the oxygen concentration leveled off with time before the glucose injection. The reasonable explanation for this phenomenon was that the biofilm was at the endogenous respiration. Previous studies have stated that oxygen is utilized at a constant rate during the endogenous phase of respiration (*3, 18*). Therefore, when the oxygen fluxes caused by the endogenous respiration and the mass transfer process in the biofilm reached a pseudo steady state, the oxygen concentration showed minimal change with time. However, the oxygen concentration had a rapid increase, which was subsequently followed by a relative plateau, usually lasting about 1 min. The rapid increase in oxygen concentration was due to the addition of oxygen associated with the injecting of substrate. A possible explanation for the plateau was that the microorganisms required a period of acclimatization prior to its consumption of the substrate, which was in relation to the decrease in oxygen spread to the oxygen microelectrode tip. On the other hand, the solution released from the peristaltic pump would pass through the sensor tip due to the inertia force, therefore resulting in the sustained oxygen concentration. As shown in Figure 2, at point B following the plateau, the oxygen concentration showed a sharp decreasing tendency due to the combination of in situ oxygen consumption by the microorganisms in biofilm and mass transfer toward the surrounding area, lasting 1−2 min. After the rapid decrease, the oxygen concentrations became stable again, indicating that another cycle of endogenous respiration was reached.

3.2. Quantification of the Biokinetic Parameters in Biofilms. In order to characterize the heterogeneous biodegradation kinetics of biofilm, the following assumptions were applied in the analysis: (1) The biofilm was at the endogenous respiration prior to the injection of substrate; (2) Glucose substrate was injected in situ at the position of oxygen microelectrode tip; and (3) Oxygen flux caused by mass transfer at point B was negligible.

Based on these assumptions, the temporary increase in OUR due to the addition of a known concentration of substrate was the maximum-value tangent at point B, $(-\mathrm{d}S_o/\mathrm{d}t)_{max}$ in the unit of mg DO/(L·s), to the decreased oxygen concentration profiles, while the term $\mathrm{OUR}/(X_f)$ is the specific oxygen uptake rate, $r_{H,ox}$ in the unit of mg DO/(g COD·d) (*6*). The OURs could be recorded by the oxygen microelectrode. X_f was the corresponding layer density of biofilm acquired by the microslicing technique. And then the $r_{H,ox}$s measured at different substrate concentrations were used to deduce the biokinetic parameters as described by Drtil et al. and Cech et al. (*3, 4*) as follows.

The Monod kinetics was commonly used to describe the substrate uptake rate by the biofilm and specific growth rate in the low substrate concentration ranges:

$$\mu_H = \mu_{H,max} \cdot \frac{S_S}{K_{H,S} + S_S} \tag{1}$$

Where μ_H was the specific growth rate, day^{-1}; $\mu_{H,max}$ was the maximum specific growth rate, day^{-1}; $K_{H,S}$ was Monod half-saturation coefficient for substrate, mg COD/L; and S_S was the substrate concentration, mg COD/L.

Based on the stoichiometric link between oxygen consumption and aerobic growth, the relationship between μ_H and $r_{H,ox}$ at concentration S_S can be expressed as follows:

$$\mu_H = \frac{Y_H}{1 - Y_H} r_{H,ox} \tag{2}$$

Where Y_H was the biomass yield coefficient, g (COD in cell)/g COD, which satisfied the following equation:

$$Y_H = 1 - \frac{OC}{S_S} \tag{3}$$

Where OC was the measured net oxygen consumption caused by the substrate biodegradation.

If a minimum of 4−5 corresponding couples of μ_H and S_S is obtained, then the biokinetic parameters of $\mu_{H,max}$ and $K_{H,S}$ can be quantified according to the Lineweaver−Burke linearization method (*19, 20*) by converting eq 1 into the following equation:

$$\frac{1}{\mu_H} = \frac{K_{H,S}}{\mu_{H,max}} \cdot \frac{1}{S_S} + \frac{1}{\mu_{H,max}} \tag{4}$$

The reliability of the biokinetic parameters depends on how closely the experimental system and the experimental procedures adhere to the assumptions of the model utilized. Therefore, each of the assumptions will be discussed separately.

1. Biofilm was at the Endogenous Respiration Prior to the Injection of Substrate. Oxygen distribution along the depth of biofilm at the retention times of 2, 24, 26, 28, and 30 h in the deionized water was checked to ensure that there was endogenous respiration present prior to the injection of substrate and to determine the retention time for which the external substrate was consumed and biofilm was at the endogenous respiration. Based on the oxygen concentration profiles in the biofilm, as shown in Figure 3, we concluded that when the retention time exceeds 24 h, the oxygen depth profiles do not change much, indicating that the biofilm was at the endogenous respiration. Therefore, to ensure that in

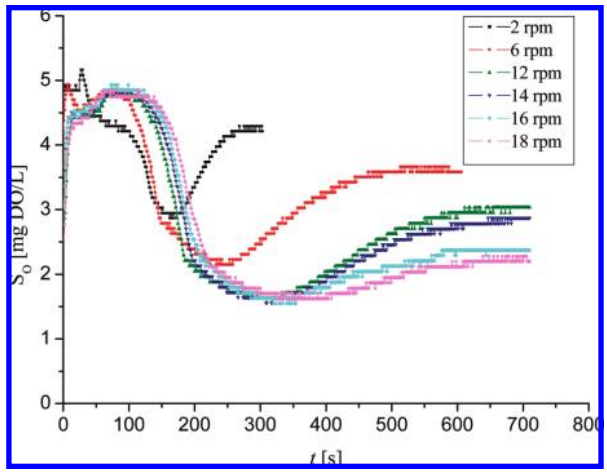

FIGURE 4. Oxygen concentration profiles with time measured at the different speed rates of peristaltic pump.

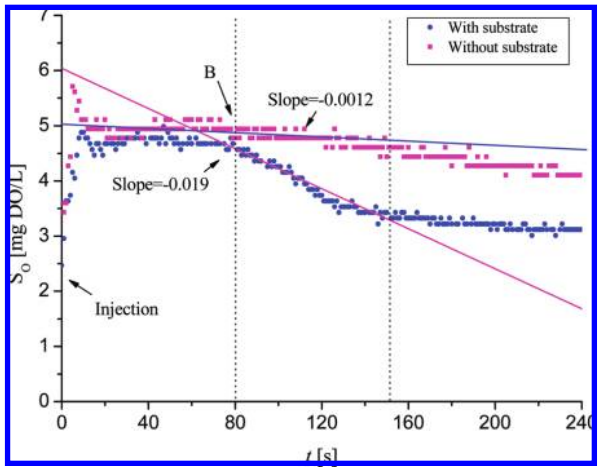

FIGURE 5. Oxygen concentration profiles with time measured (a) with or (b) without the glucose in the injection solution.

our measurements biofilm was at the endogenous respiration, we used 26 h for the retention time.

2. Glucose Substrate Was Injected in Situ at the Position of Oxygen Microelectrode Tip. The requirement can be approximately satisfied by adjusting the speed of the peristaltic pump to the extent that the measured S_O-t profiles have minimal difference with the speed increase. This indicates that the mass transfer limitation between the locations of two micropipette tips can be negligible. We measured the oxygen profiles at varying speeds of 2, 6, 12, 14, 16, and 18 rpm, resulting in the total injection volume of 10, 30, 60, 70, 80, and 90 μL in 6 s, and found that the profiles measured were indeed almost identical (Figure 4, with glucose concentration of 4.8 mg/L) at the speed of 16 and 18 rpm. Furthermore, the measured oxygen profiles showed an increasing tendency followed in the bottom of the profiles. We attributed this phenomenon to the oxygen transfer from other areas to the sensor tip due to the minimal amount of substrate injected. However, high speed associated with corresponding maximal flow rate may lead to the destruction of the biofilm structure; therefore, the optimal speed of 16 rpm was applied throughout the experiment.

3. Oxygen Concentration Gradient Caused by Mass Transfer at Point B Was Negligible. In order to weigh the oxygen gradient effect caused by mass transfer on the calculation of OUR at the specified substrate concentration of S_S, the deionized water without glucose was injected into the biofilm. The comparison between with and without the substrate is presented in Figure 5. Previous studies revealed that the

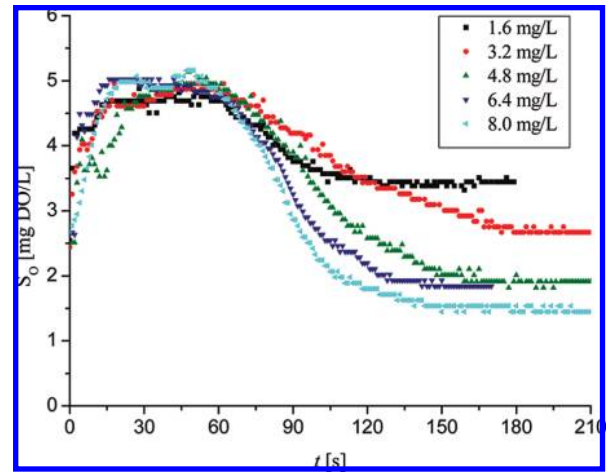

FIGURE 6. Oxygen concentration profiles with time measured at a series of glucose concentrations in the injection solution.

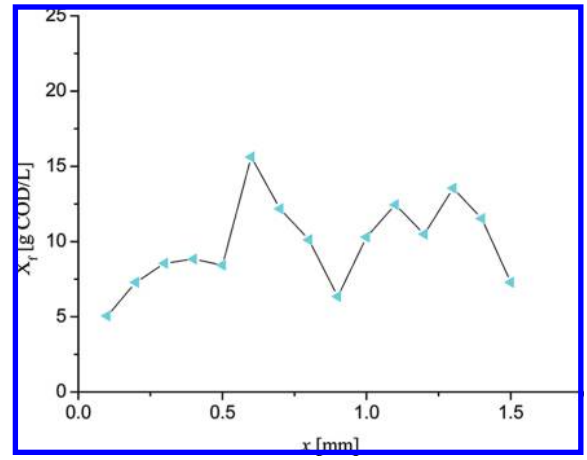

FIGURE 7. Spatial distribution of layer densities in biofilm.

effective diffusivity of oxygen decreased toward the bottom of the biofilm (*21, 22*)., To make the comparison more typical, we chose the S_O-t profile without the substrate at the biofilm surface layer of 0.4 mm for comparison because the oxygen gradient caused by mass transfer is relatively large. In contrast, the microbial activities were usually found to decrease with the biofilm depth (*33*), therefore, the S_O-t profile with glucose concentration of 1.6 mg COD/L at the biofilm deep layer of 1.1 mm was chosen for comparison. However, in such case of adverse conditions, the oxygen concentration gradient caused by mass transfer at point B was quantified to be -0.0012 mg DO/(L·s), which was still one magnitude smaller compared to the maximum gradient of -0.019 mg DO/(L·s) in combination with the microbial activities. Therefore, it is reasonable that we assume the oxygen concentration gradient caused by mass transfer at point B can be neglected.

Furthermore, we still found that during the two dashed lines period as shown in Figure 5, which indicated the time for the biodegradation of the injected S_S, the mean oxygen decreasing gradient without substrate addition was calculated to be -0.0044 mg DO/(L·s), resulting in the decrease of 0.31 mg DO/L in the oxygen concentration. It meant that a net oxygen decrease of 0.31 mg DO/L was caused by mass transfer during the period of substrate biodegradation, which is not much smaller compared with the net oxygen decrease caused by the combination of the biodegradation of the injected substrate and the mass transfer (equal to 1.25 mg DO/L as shown in Figure 5), especially in the case of the low substrate concentration. Therefore, the net oxygen decrease caused

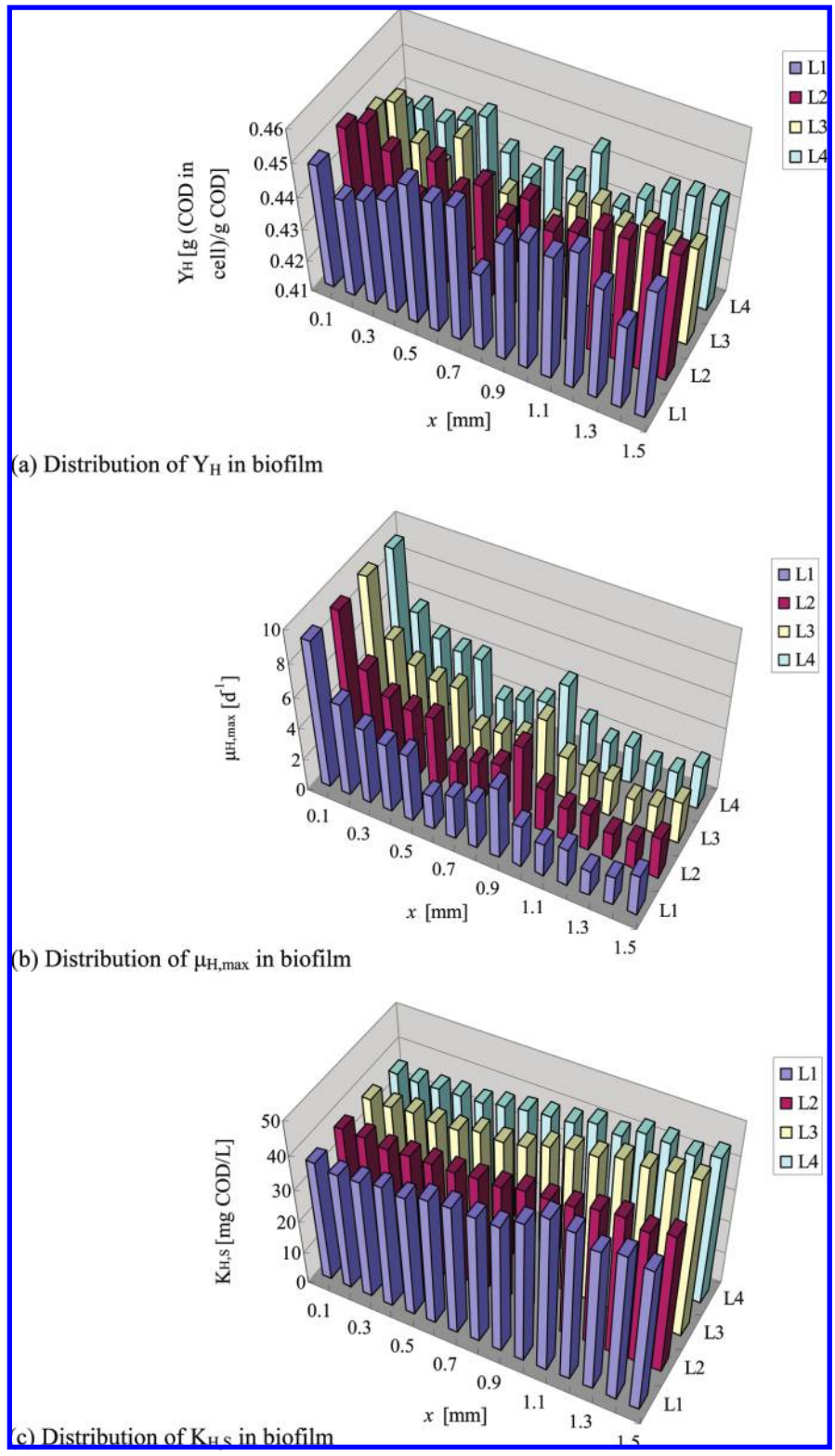

FIGURE 8. Distribution of biokinetic parameters (a) Y_H, (b) $\mu_{H,max}$, and (c) $K_{H,S}$ at four locations in the biofilm. L1, L2, L3, and L4 was at the vertexes of a square with a side length of 10 mm.

by mass transfer has been taken into consideration in the calculation of OC.

Figure 6 plotted an example of the measured oxygen profiles with time at the biofilm depth of 1.2 mm with the injection of a series of known glucose concentrations. The layer densities of biofilm used for the modeling were plotted in Figure 7. Based on the figures, the detailed calculation of biokinetic parameters is listed in Table 2.

3.3. Spatial Distribution of Biokinetic Parameters in Biofilm. Figure 8 illustrates the spatial distribution of biokinetic parameters in the biofilm, based on the collection of 300 oxygen profiles with time. It should be noted that the layer densities of biofilm, as shown in Figure 7, were coupled to deduce the stratification of biokinetic parameters.

Kinetic characterization of biological processes via batch respirometry requires an accurate estimate of the biomass

TABLE 2. Calculation of Biokinetic Parameters at the Biofilm depth of 1.2 mm (X_f = 10.5 g COD/L)

S_S (mg COD/L)	OUR (mg DO/(L·s))	$r_{H,ox}$ (mg DO/(g COD·d))	μ_H (day^{-1})	Y_H (g (COD in cell)/g COD)	$\mu_{H,max}$ (day^{-1})	$K_{H,s}$ (mg COD/L)
1.6	0.0151	116.5	0.1067	0.413		
3.2	0.0266	205.2	0.1880	0.434		
4.8	0.0433	334.8	0.3060	0.429		
6.4	0.0555	428.1	0.3922	0.491		
8.0	0.0656	506.1	0.4635	0.545		
calculated: $1/\mu_H = 14.594/S_S + 0.3683$				0.462 ± 0.049	2.71	39.63

yield coefficient, as it provides the stoichiometric link between biomass synthesis, substrate consumption and oxygen uptake (*23*). However, to the best of our knowledge, few studies have reported the Y_H measured in the attached growth systems because it was and still is difficult to derive if the mass transfer limitation is taken into consideration. Tsuneda et al. (*24*) introduced a step change experiment to quantify biokinetic parameters ($\mu_{H,max}$, $K_{H,S}$, Y_H) in a three-phase fluidized bed biofilm reactor, however, where the substrate transfer in biofilms was ignored. In modeling the biofilm process, the simplest and most commonly applied method was to use the Y_H measured in suspended cultures to model and predict microbial growth in biofilms (*25*−*27*). In this study, we acquired the approximate link between the substrate consumption and the oxygen uptake according to the oxygen profile with time at a known substrate concentration. The measured Y_H of biofilm was within the 0.437−0.449 g (COD in cell)/g COD range, which only had a slight difference and no regular change at the various locations of the biofilm. These values were noted to be smaller than the Y_H of activated sludge (0.67 g (COD in cell)/g COD at 20 °C) recommended by the IWA (International Water Association) (*30*). In Goel et al.'s study, Y_H was found to be dependent on the type of carbon substrate, which resulted in different intracellular storage compounds (*31*). Compared with the Y_H of 0.58−0.50 g (COD in cell)/g COD in the case of glucose as substrate measured in the activated sludge system (*31*), the measured values in this study were still smaller. We attributed it to the less microbial activities in the attached growth system compared with the suspended growth system. We also found the values obtained from this experiment were reasonable and adjacent to the Y_H of 0.45 g (COD in cell)/g COD adopted by many previous studies on biofilm kinetic modeling (*7, 28, 29*).

Furthermore, the difficulty in determining of Y_H in biofilm led to the unreachability of $\mu_{H,max}$, therefore, the expression of $\mu_{H,max}/Y_H$ was usually measured as a whole (*20, 28, 32*). On the other hand, using the $\mu_{H,max}$ measured in the suspended cultures to model and predict the microbial growth in biofilms was also common (*26, 27*), although it is not scientific. Figure 8 shows the stratified distribution of $\mu_{H,max}$ measured by the new approach. It can be well seen that the $\mu_{H,max}$ varied from 9.18 $days^{-1}$ at the surface layer of the biofilm to 1.69 day^{-1} at the substratum layer of the biofilm with a decrease of 80%, wherein a sharp decrease in $\mu_{H,max}$ occurred in the surface 300 μm of biofilm (from 9.18 to 4.8 day^{-1}), indicating that higher microbial activities exited in the layer. Below the depth of 300 μm, a relatively mild decrease with a little fluctuation in the $\mu_{H,max}$ were found. The $\mu_{H,max}$ at the substratum layer of 600 μm in the biofilm (1.6−2.6 day^{-1}) was closer to the values obtained from three-phase fluidized bed biofilm reactors in Tsuneda et al.'s study (*24*) (within the range of 1.2−2.0 day^{-1}). The decrease in $\mu_{H,max}$ toward the bottom of biofilm can be explained in two ways. One was the reduction of biomass activity, which was supported by the experimental evidence in the study of Zhang et al. (*33*) that the ratio of living cells to total biomass decreases from about 72−91% in the top biofilm layers to 31−39% in the bottom layers. Another explanation was that the fast growing microorganisms would tend to predominate near the surface, whereas slow growers would be deeper inside the film, scavenging substrate from the fast growers, which accorded with the theoretical prediction by Wanner and Gujer (*34*).

A close relationship has been reported between the biokinetic parameters, in particular Monod half-saturation coefficient, and the mass transport limitation in attached growth systems (*9, 19*). As shown in Figure 8, the measured $K_{H,S}$ was increased from 37 mg COD/L at the surface layer of the biofilm to 45 mg COD/L at the substratum layer of the biofilm, indicating larger mass transport limitations with the penetration of biofilm. Most $K_{H,S}$ were larger than the values for other biomass grown in suspension (10 mg/L by Cech et al. (*4*); 20 mg/L recommended by the IWA (*30*)). This is in approximate agreement with the conclusion reported by Pérez et al. (*35*) that the effect of mass transport limitations is reflected by half-velocity coefficients in the Monod expression which are 1 order of magnitude greater for activated sludge flocs than those reported for single suspended cells. The measured $K_{H,S}$ was in the larger part of the range of $K_{H,S}$ reported in previous biofilm studies (10 mg/L by Horn and Hempel (*36*); 17.41 mg/L by Hirata et al. (*20*); 22 mg/L by Beyenal et al. (*25*); 63−84 mg/L by Tsuneda et al. (*24*)).

As shown in Figure 8, we also found that the distribution of biokinetic parameters was less heterogeneous in the horizontal direction at the same depth compared with the high heterogeneity in the biofilm depth.

Acknowledgments

We thank the Chinese Natural Science Foundation (50478009), the 973 Chinese−Canadian Cooperation Project (2005-CB724901), and the Ph.D. Programs Foundation of the Ministry of Education of China (No. 20040003040). We also thank the help from the department of biology, Tsinghua University, for the experiment of microslicing.

Literature Cited

(1) Bishop, P. L. Biofilm structure and kinetics. *Water Sci. Technol.* **1995**, *36*, 287–294.
(2) Riefler, R. G.; Smets, B. F. Comparison of a type curve and a least-squared errors method to estimate biofilm kinetic parameters. *Water Res.* **2003**, *37*, 3279–3285.
(3) Drtil, M.; Németh, P.; Bodík, I. Kinetic constants of nitrification. *Water Res.* **1993**, *27*, 35–39.
(4) Cech, J. S.; Chudoba, J.; Grau, P. Determination of kinetics constants of activated sludge microorganisms. *Water Sci. Technol.* **1984**, *17* (2/3), 259–272.
(5) Kim, I. S.; Kim, S. Y.; Jang, A. Activity monitoring for nitrifying bacteria by fluorescence in situ hybridization and respirometry. *Environ. Monit. Assess.* **2001**, *70*, 223–231.
(6) Beyenal, H.; Chen, S. N.; Lewandowski, Z. The double substrate growth kinetics of *Pseudomonas aeruginosa*. *Enzyme Microb. Technol.* **2003**, *32*, 92–98.
(7) Riefler, R. G.; Ahlfeld, D. P.; Smets, B. F. Respirometric assay for biofilm kinetics estimation: parameter identifiability and retrievability. *Biotechnol. Bioeng.* **1998**, *57* (1), 35–45.
(8) Carvallo, L.; Carrera, J.; Chamy, R. Nitrifying activity monitoring and kinetic parameters determination in a biofilm airlift reactor by respirometry. *Biotechnol. Lett.* **2002**, *24*, 2063–2066.

(9) Plattes, M.; Fiorelli, D.; Gille, S.; Girard, C.; Henry, E.; Minette, F.; O'Nagy, O.; Schosseler, P. M. Modelling and dynamic simulation of a moving bed bioreactor using respirometry for the estimation of kinetic parameters. *Biochem. Eng. J.* **2007**, *33*, 253–259.
(10) Bishop, P. L.; Rittmann, B. E. Modelling heterogeneity in biofilms: Report of the discussion session. *Water Sci. Technol.* **1995**, *32* (8), 263–265.
(11) Zhang, T. C.; Fu, Y.-C.; Bishop, P. L. Competition for substrate and space in biofilms. *Water Environ. Res.* **1995**, *67* (6), 992–1002.
(12) Whalen, W. J.; Bungay, H. R.; Sanders, W. M. Microelectrode determination of oxygen profiles in microbial slime systems. *Environ. Sci. Technol.* **1969**, *3* (12), 1297–1298.
(13) Hooijmans, C. M.; Geraats, S. G. M.; Luyben, K. Ch. A. M. Use of an oxygen microsensor for the determination of intrinsic kinetic parameters of an immobilized oxygen reducing enzyme. *Biotechnol. Bioeng.* **1990**, *35* (11), 1078–1087.
(14) Yurt, N.; Beyenal, H.; Sears, J.; Lewandowski, Z. Quantifying selected growth parameters of *Leptothrix discophora* SP-6 in biofilms from oxygen concentration profiles. *Chem. Eng. Sci.* **2003**, *58*, 4557–4566.
(15) Zhou, X.-H.; Shi, H.-C.; Cai, Q.; He, M.; Wu, Y.-X. Function of self-forming dynamic membrane and biokinetic parameters' determination by microelectrode. *Water Res.* **2008**, *42*, 2369–2376.
(16) Yu, T.; Bishop, P. L. Stratification of microbial metabolic processes and redox potential change in an aerobic biofilm studied using microelectrodes. *Water Sci. Technol.* **1998**, *37*, 195–198.
(17) Jensen, K.; Revsbech, N. P.; Nielsen, L. P. Microscale distribution of nitrification activity in sediment determined with a shielded microsensor for nitrate. *Appl. Environ. Microbiol.* **1993**, *59* (10), 3287–3296.
(18) Avcioglu, E.; Orhon, D.; Sözen, S. A new method for the assessment of heterotrophic endogenous respiration rate under aerobic and anoxic conditions. *Water Sci. Technol.* **1998**, *38* (8/9), 95–103.
(19) Chen, K.-C.; Wu, J.-Y.; Yang, W.-B.; Hwang, S-C.J. Evaluation of effective diffusion coefficient and intrinsic kinetic parameters on azo dye biodegradation using PVA-immobilized cell beads. *Biotechnol. Bioeng.* **2003**, *83* (7), 821–832.
(20) Hirata, A.; Takemoto, T.; Ogawa, K.; Auresenia, J.; Tsuneda, S. Evaluation of kinetic parameters of biochemical reaction in three-phase fluidized bed biofilm reactor for wastewater treatment. *Biochem. Eng. J.* **2000**, *5*, 165–171.
(21) Fu, Y.-C.; Zhang, T. C.; Bishop, P. L. Determination of effective oxygen diffusivity in biofilms growth in a completely mixed biodrum reactor. *Water Sci. Technol.* **1994**, *29* (10/11), 455–462.
(22) Beyenal, H.; Tanyolaç, A.; Lewandowski, Z. Measurement of local effective diffusivity in heterogeneous biofilms. *Water Sci. Technol.* **1998**, *38* (8/9), 171–178.
(23) Chandran, K.; Smets, B. F. Estimating biomass yield coefficients for autotrophic ammonia and nitrite oxidation from batch respirograms. *Water Res.* **2001**, *35* (13), 3153–3156.
(24) Tsuneda, S.; Auresenia, J.; Inoue, Y.; Hashimoto, Y.; Hirata, A. Kinetic model for dynamic response of three-phase fluidized bed biofilm reactor for wastewater treatment. *Biochem. Eng. J.* **2002**, *10*, 31–37.
(25) Beyenal, H.; Tanyolaç, A. A mathematical model for hollow fiber biofilm reactors. *Chem. Eng. J.* **1994**, *56*, B53−B59.
(26) Hsien, T.-Y.; Lin, Y-H. Biodegradation of phenolic wastewater in a fixed biofilm reactor. *Biochem. Eng. J.* **2005**, *27*, 95–103.
(27) Tanyolaç, A.; Beyenal, H. Prediction of substrate consumption rate, average biofilm density and active thickness for a thin spherical biofilm at pseudo-steady state. *Biochem. Eng. J.* **1998**, *2*, 207–216.
(28) Rittmann, B. E.; Crawford, L.; Tuck, C. K.; Namkung, E. In-situ determination of kinetic parameters for biofilms: isolation and characterization of oligotrophic biofilms. *Biotechnol. Bioengin.* **1986**, *28*, 1753–1760.
(29) Nicolella, C. N.; Pavasant, P.; Livingston, A. G. Substrate counterdiffusion and reaction in membrane-attached biofilms: mathematical analysis of rate limiting mechanisms. *Chem. Eng. Sci.* **2000**, *55*, 1385–1398.
(30) *IWA Task Group on Mathematical Modeling for Design and Operation of Biological Wastewater Treatment. Activated Sludge Models ASM1, ASM2, ASM2D and ASM3*; IWA Publishing: London, England, 2000.
(31) Goel, R.; Mino, T.; Satoh, H.; Matsuo, T. Intracellular storage compounds, oxygen uptake rates and biomass yield with readily and slowly degradable substrates. *Water Sci. Technol.* **1998**, *38* (8/9), 85–93.
(32) Tsuneda, S.; Auresenia, J.; Morise, T.; Hirata, A. Dynamic modeling and simulation of a three-phase fluidized bed batch process for wastewater treatment. *Process Biochem.* **2002**, *38*, 599–604.
(33) Zhang, T. C.; Bishop, P. L. Density, porosity and pore structure of biofilms. *Water Res.* **1994**, *28*, 2267–2277.
(34) Wanner, O.; Gujer, W. Competition in biofilms. *Water Sci. Technol.* **1984**, *17*, 27–44.
(35) Pérez, J.; Picioreanu, C.; van Loosdrecht, M. Modeling biofilm and floc diffusion processes based on analytical solution of reaction-diffusion equations. *Water Res.* **2005**, *39* (7), 1311–1323.
(36) Horn, H.; Hempel, D. C. Growth and decay in an auto-/heterotrophic biofilm. *Water Res.* **1997**, *31* (9), 2243–2252.
(37) China EPA. *Analysis Methods for Water and Wastewater (In Chinese)*. 3rd ed.; Chinese Environmental Science Press.: Beijing. China., 1997.
(38) Taylor, D. G.; Breen, A.; Bishop, P. L. Determination of phenol-degrader distribution in biofilms using gene probes. *Water Res.* **1997**, *31*, 119–129.

ES802373Q